

RESEARCH ARTICLE | JUNE 01 1995

## Vibrational numbering and potential of the $c\ ^3\Sigma^+$ state of NaK determined from the $c\ ^3\Sigma^+ \rightarrow a\ ^3\Sigma^+$ transition

P. Kowalczyk; N. Sadeghi



*J. Chem. Phys.* 102, 8321–8327 (1995)

<https://doi.org/10.1063/1.468824>



View  
Online



Export  
Citation

CrossMark

### Articles You May Be Interested In

The  $a\ ^3\Sigma^+$  state of NaK. High resolution spectroscopy using laser-induced fluorescence (LIF)

*J. Chem. Phys.* (July 2008)

An inversion procedure for oscillatory continuum spectra: Method and application to NaK

*J. Chem. Phys.* (October 1988)

Experimental studies of the NaK  $1\ ^3\Delta$  state

*J. Chem. Phys.* (November 2000)

Downloaded from [http://pubs.aip.org/aip/jcp/article-pdf/102/21/8321/9434926/8321\\_1\\_online.pdf](http://pubs.aip.org/aip/jcp/article-pdf/102/21/8321/9434926/8321_1_online.pdf)



The Journal of Chemical Physics

Special Topic: Adhesion and Friction

Submit Today!

# Vibrational numbering and potential of the $c\ ^3\Sigma^+$ state of NaK determined from the $c\ ^3\Sigma^+ \rightarrow a\ ^3\Sigma^+$ transition

P. Kowalczyk<sup>a)</sup> and N. Sadeghi

Laboratoire de Spectrométrie Physique (CNRS URA 08), Université Joseph-Fourier/Grenoble I, B.P. 87, 38402 Saint-Martin-d'Hères, Cédex, France

(Received 30 August 1994; accepted 23 February 1995)

We report the observation of the  $c\ ^3\Sigma^+ \rightarrow a\ ^3\Sigma^+$  emission in NaK following excitation of single rovibronic levels in the  $c\ ^3\Sigma^+$  state. The dispersed fluorescence displays both diffuse and discrete features. The characteristic reflection structure of the bound-free spectra permits a direct, unambiguous assignment of the vibrational numbering in the  $c\ ^3\Sigma^+$  state: The  $v=20$  level is the first vibrational level of  $c\ ^3\Sigma^+$  lying above  $v=0$  in the  $B\ ^1\Pi$  state. The  $c\ ^3\Sigma^+$  state potential curve is determined from bound-free parts of the observed spectra with the inversion procedure of LeRoy *et al.* [J. Chem. Phys. **89**, 4564 (1988)]; its most important parameters are  $T_e = 15\,857 \pm 15\text{ cm}^{-1}$  and  $R_e = 0.445 \pm 0.001\text{ nm}$ . © 1995 American Institute of Physics.

## INTRODUCTION

The alkali dimers play a special role in quantum chemistry as prototypes for a broader range of diatomics, since accurate quantum mechanical calculations are feasible for them. As their ground states are of singlet symmetry, spectroscopy of this important class of molecules has been long limited to transitions between electronic singlet states. However, high-resolution laser techniques developed in recent decades have allowed the use of perturbations between singlet and triplet levels as a gateway to the triplet manifold. The heteronuclear alkali dimers are particularly suitable for such studies since the lower symmetry of these molecules enlarges the possibilities of interaction between molecular states beyond those present in the homonuclear dimers.

The  $c\ ^3\Sigma^+$  state of NaK is one of the states most studied by this method. It interacts strongly with the  $B\ ^1\Pi$  state (see Fig. 1) and in its perturbed parts, where the vibrational levels become superpositions of singlet and triplet levels, can be easily accessed from the ground  $X\ ^1\Sigma^+$  state. The “spin-forbidden”  $c\ ^3\Sigma^+ \leftarrow X\ ^1\Sigma^+$  transition has been observed under high resolution in several experiments: in vacuum cells,<sup>1–5</sup> heat-pipe ovens,<sup>6–8</sup> and in molecular beam conditions.<sup>9–11</sup> The  $c\ ^3\Sigma^+$  state has been well characterized for vibrational levels which are perturbed by the  $B\ ^1\Pi$  state, i.e., in the energy range approximately 17 100–17 800  $\text{cm}^{-1}$  above the bottom of the ground  $X\ ^1\Sigma^+$  state potential. However, the  $c$  state potential well is deeper than that of the  $B$  state, and its lowest levels are inaccessible to experimental observation by the method mentioned earlier. As a result, the parameters describing the bottom of the  $c\ ^3\Sigma^+$  state could only be estimated by extrapolation of the molecular constants of the directly observed high vibrational levels and the resulting RKR potential curve was not highly reliable. In fact, even the vibrational numbering in the  $c$  state was in question; if we label by  $v_0$  the first vibrational level of the  $c\ ^3\Sigma^+$  state lying above  $v=0$  in the  $B\ ^1\Pi$  state, various authors proposed  $v_0$  between 12 (Ref. 7) and 20 (Ref. 3). The

paper by Kowalczyk *et al.*<sup>5</sup> discussed this problem in more detail and recommended the value  $v_0=16$ , based on the measured matrix elements of the  $B-c$  perturbation for different levels in  $^{23}\text{Na}^{39}\text{K}$  and  $^{23}\text{Na}^{41}\text{K}$  molecules.

To remove this ambiguity concerning the vibrational numbering, we decided to study the  $c\ ^3\Sigma^+ \rightarrow a\ ^3\Sigma^+$  emission spectra following excitation of single rovibronic levels in the  $c$  state. The  $a\ ^3\Sigma^+$  state is unbound except for a shallow van der Waals minimum at large internuclear separation, and its potential curve is known, both in the bound and in the repulsive parts.<sup>12–14</sup> The resulting  $c \rightarrow a$  spectra should consist predominantly of oscillatory continua. We expected that the number of oscillations and positions of maxima and minima in these continua would provide information about the whole shape of the  $c\ ^3\Sigma^+$  state potential and, in particular, the correct vibrational numbering.

## EXPERIMENT

The experimental setup and equipment used here has been mostly described elsewhere.<sup>2–5</sup> Briefly, NaK molecules were formed in a Pyrex cell containing approximately 7:3 mixture (by weight) of potassium and sodium and heated to 220 °C. Fluorescence of NaK was excited by a beam from a single mode ring dye laser (Coherent CR 699-21) working on rhodamine 6G with typically 300 mW cw output power. The dye laser wavelength was measured with a homebuilt wavemeter.<sup>3,15</sup> The molecular fluorescence observed at right angles to the incident laser beam was dispersed by a 0.6 m grating monochromator (Jobin-Yvon HRS, 600 grooves/mm, blazed at 1  $\mu\text{m}$ ) with a spectral resolution full width at half-maximum (FWHM) of 0.35 nm. The spectra were recorded with a back illuminated CCD detector (CCD-500B, Princeton Instruments, spectral range 350–1100 nm) interfaced to a personal computer for storage and further treatment of the data. The wavelengths of the observed fluorescence were calibrated against the emission spectra of neon and mercury.<sup>16</sup> The spectral response of the whole detection system was determined by using a tungsten filament lamp operated at  $T=1400\text{ °C}$  which was considered to be a black-body radiation source.

<sup>a)</sup>On leave from Institute of Experimental Physics, Warsaw University, ul.Hoza 69, 00-681 Warsaw, Poland.

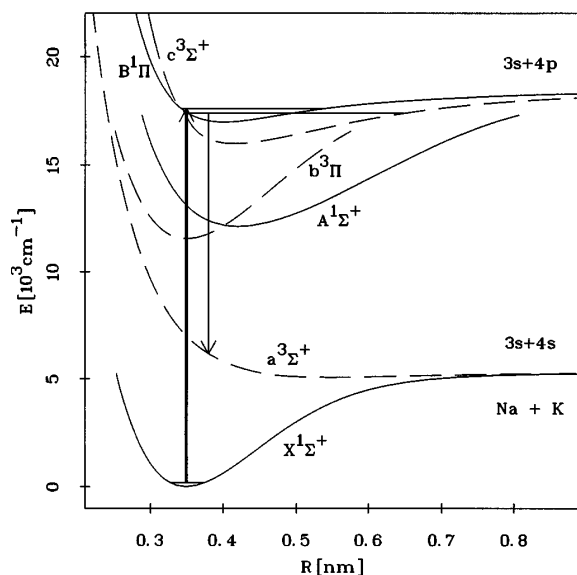


FIG. 1. Potential energy curves of the NaK molecule for states corresponding to the two lowest  $\text{Na}(3^2S) + \text{K}(4^2S)$  and  $\text{Na}(3^2S) + \text{K}(4^2P)$  asymptotes. The arrows show schematically the excitation of the mutually perturbed levels in the  $B^1\Pi$  and  $c^3\Sigma^+$  states from the ground  $X^1\Sigma^+$  state followed by fluorescence to the  $a^3\Sigma^+$  state.

## RESULTS

In the present experiment we selectively excited either of the two components in the four pairs of strongly interacting

rovibronic levels in the  $c^3\Sigma^+$  and  $B^1\Pi$  states of  $^{23}\text{Na}^{39}\text{K}$  (Refs. 3 and 10) (Fig. 1):  $v_c = v_0 + 5$ ,  $J_c^e = 13$  and  $v_B = 4$ ,  $J_B^e = 13$  (excitation from  $v'' = 0$ ,  $J'' = 14$  in the ground  $X^1\Sigma^+$  state at 580.704 and 580.693 nm, respectively);  $v_c = v_0 + 8$ ,  $J_c^f = 31$  and  $v_B = 6$ ,  $J_B^f = 31$  (excitation from  $v'' = 0$ ,  $J'' = 31$  at 577.544 and 577.554 nm);  $v_c = v_0 + 11$ ,  $J_c^e = 46$  and  $v_B = 8$ ,  $J_B^e = 46$  (excitation from  $v'' = 0$ ,  $J'' = 45$  at 575.099 and 575.120 nm);  $v_c = v_0 + 13$ ,  $J_c^f = 31$  and  $v_B = 10$ ,  $J_B^f = 31$  (excitation from  $v'' = 0$ ,  $J'' = 31$  at 570.917 and 570.939 nm) where the superscripts  $e$  or  $f$  denote the parity of levels. For each excitation we observed the dispersed fluorescence spectrum of the  $c^3\Sigma^+ \rightarrow a^3\Sigma^+$  transition. As an example, Figs. 2 and 3 show the spectra following excitation of the  $v_c = v_0 + 5$ ,  $J_c^e = 13$  and  $v_c = v_0 + 13$ ,  $J_c^f = 31$  levels. The spectra consist of a dominant modulated continuum, which belongs to transitions to the repulsive part of the  $a^3\Sigma^+$  potential curve, and few discrete lines corresponding to transitions to bound states in a shallow well of this potential (only partially resolved given the poor spectral resolution in this experiment; high resolution spectra of these regions have been reported in Ref. 3). The observed bound-free part of the emission is characterized by a regular oscillatory structure. With higher excitation energies the number of oscillations increases and the onset of the spectra at high frequencies shifts to the blue. However, the position of the first maximum at the low frequency side of the spectra varies very little, indicating that the upper and lower state potential curves are nearly parallel for small internuclear separations.

We attempted to simulate the experimentally observed bound-free spectra by a rigorous quantum mechanical

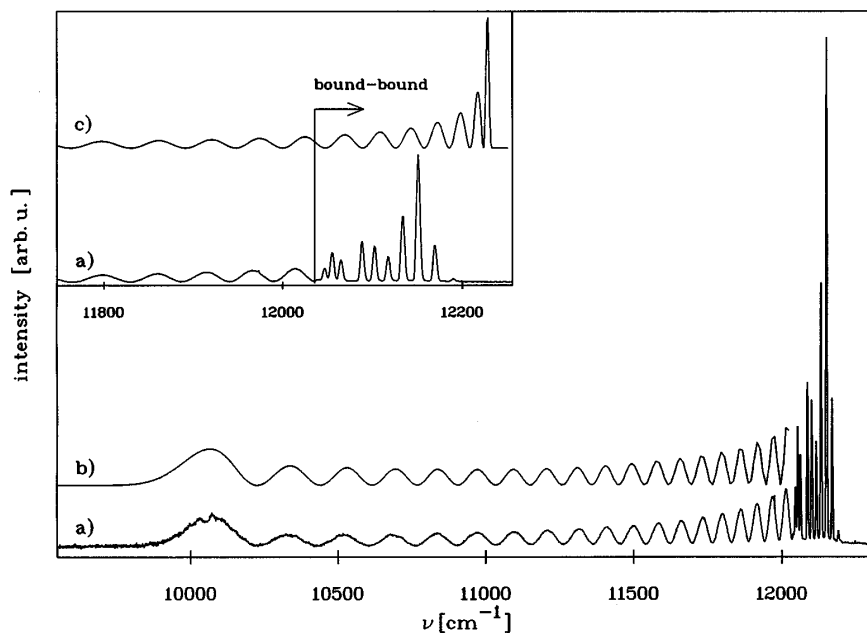


FIG. 2. (a) The  $c^3\Sigma^+ \rightarrow a^3\Sigma^+$  emission from the  $v_c = v_0 + 5$ ,  $J_c = 13$  level (excitation at 580.704 nm). The spectral region containing a partially resolved bound-bound fluorescence is enlarged in the inset. (b) Simulation of the bound-free part of the spectrum with the  $c^3\Sigma^+$  state potential from Table I and the  $a^3\Sigma^+$  state potential combining the RKR curve with formula (2). (c) High frequency part of the spectrum simulated using the completely repulsive  $a^3\Sigma^+$  state potential (see the text).

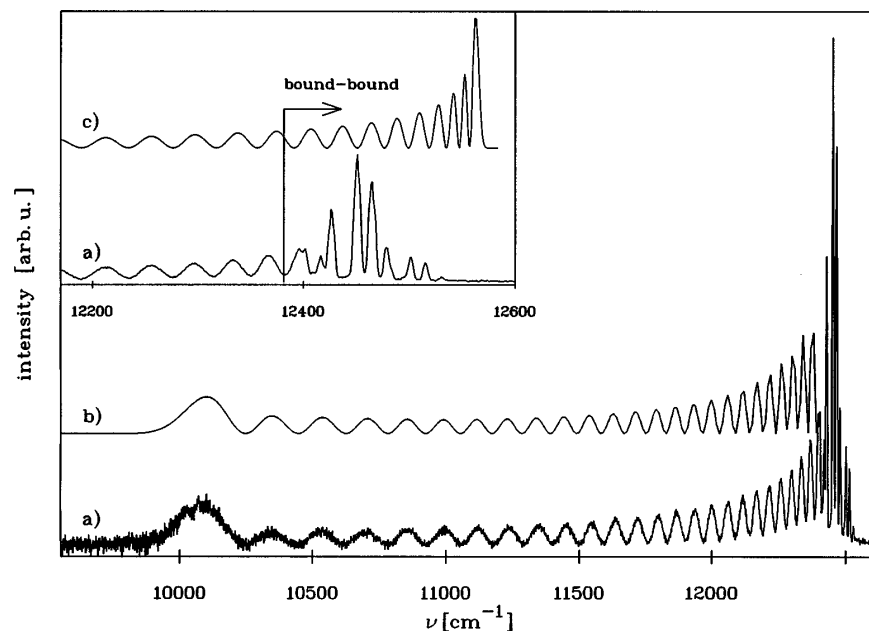


FIG. 3. The same as Fig. 2, for emission from the  $v_c=v_0+13$ ,  $J_c=31$  level (excitation at 570.917 nm).

method, using a computer code developed in our laboratory. In brief, with specified potential curves of the upper and lower states as an input, the program calculates the discrete and continuum wave functions by the Numerov–Cooley method<sup>17</sup> and transforms the overlap integrals into the fluorescence intensity. The performance of the program was verified by comparison with the BOUND–FREE program of Herman and Sando.<sup>18</sup> Initially, the potential curves used for simulations were the combined RKR and repulsive wall potential for the  $a^3\Sigma^+$  state<sup>12–14</sup> and the RKR potential corresponding to the vibrational numbering with  $v_0=16$  for the  $c^3\Sigma^+$  state.<sup>10</sup> To our surprise, the simulated spectra differed from the experimental ones not only in the positions of the maxima and minima but also in the general appearance: instead of the observed regular oscillatory pattern we obtained rather complicated structures with irregularly changing intensities.

At this point it may be convenient to invoke a simple semiclassical picture, useful for a qualitative analysis of spectra. As has been outlined in detail by Mulliken<sup>19</sup> and Tellinghuisen,<sup>20</sup> the spectral shape of a band corresponding to a bound–free transition is simply related to the nature of the Mulliken difference potential, defined as

$$V_M(R) = E(v', J') - [V'(R) - V''(R)]. \quad (1)$$

When  $V_M(R)$  is monotonic, a contribution to the spectrum for each frequency  $\omega$  comes from a single point (the so-called Condon point)  $R_C$  for which  $E(v', J') - \hbar\omega = V_M(R_C)$ . Then the band displays a *reflection structure*, i.e., regular oscillations in the resulting spectrum simply reflect the radial probability density for the initial level  $v'$ . When

$V_M(R)$  has one or more extrema, the band displays a more complicated *interference structure*. A constructive or destructive interference of contributions from several Condon points in some (or the whole) of the frequency range introduces, in this case, additional modulation to the spectral distribution. The simple oscillatory pattern observed in all our experimental spectra strongly suggests a reflection structure. However, the described above potentials for the  $c^3\Sigma^+$  and  $a^3\Sigma^+$  states used in the simulations, give the Mulliken difference potential with a maximum (Fig. 4) and therefore the calculated spectra display a more complicated interference structure. To solve this problem we initially tried to deform the  $a^3\Sigma^+$  state potential curve from Ref. 14 by making the repulsive wall steeper, however, we were not able to obtain correct simulations before making the potential physically unacceptable. In addition, the original potential of the  $a^3\Sigma^+$  state allowed the experimental spectra of the  $b^3\Pi \rightarrow a^3\Sigma^+$  and  $d^3\Pi \rightarrow a^3\Sigma^+$  transitions to be reproduced<sup>14</sup> and should be accepted as reliable. Therefore we concluded that the  $c^3\Sigma^+$  state potential must be in question—both its shape and, consequently, the vibrational numbering in the  $c$  state.

Instead of a trial-and-error approach, we applied the inversion procedure proposed by LeRoy *et al.*<sup>21</sup> to generate the  $c^3\Sigma^+$  state potential. This method allows one to determine the potential well of the initial bound state from a knowledge of the repulsive potential curve of the final state and of the positions of the maxima and minima in the oscillatory spectrum, provided the spectrum is of a reflection type. We generated the  $c^3\Sigma^+$  state potential from all eight experimentally available bound–free spectra. The potentials obtained were

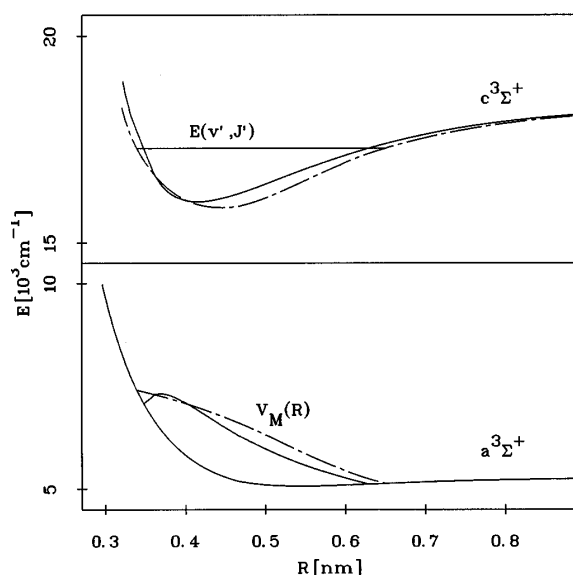


FIG. 4. The potential curves of the  $a^3\Sigma^+$  state (from Refs. 12–14) and those of the  $c^3\Sigma^+$  state, proposed in Ref. 10,  $v_0=16$  (solid line) and from the present work (dashed–dotted line). The Mulliken difference potentials  $V_M(R)$  related to both upper state potentials are displayed for transitions from the  $E(v'=v_0+5, J'=13)$  level.

nearly identical (with a dispersion in  $T_e$  of  $30\text{ cm}^{-1}$  and in  $R_e$  of only  $0.002\text{ nm}$ ), showing that the inversion procedure worked correctly; for further consideration we employed the average of these potentials, given in Table I. The “inverted” potential curve of the  $c^3\Sigma^+$  state is also displayed in Fig. 4. As can be seen, the corresponding Mulliken difference potential for the  $c^3\Sigma^+ \rightarrow a^3\Sigma^+$  transition is now monotonic, in agreement with the appearance of the experimental spectrum.

The vibrational numbering in the  $c^3\Sigma^+$  state remained still unclear at this stage of the analysis. The inversion procedure used here is not sensitive to the vibrational quantum number of the bound level, as discussed by LeRoy *et al.*<sup>21</sup> The reflection structure of the observed spectra suggested that the vibrational numbering can be obtained simply by counting the number of maxima in the spectra, each maximum being associated with one extremum of the upper state vibrational wave function. However, one has to remember that the experimental spectra become discrete at the high frequency end and the intensity extrema corresponding to the lowest final state energies cannot be clearly resolved. Essentially, the oscillatory pattern continues into the bound–bound part of the spectrum in the form of the Franck–Condon envelope of the discrete transitions. However, the actual shape of the envelope may be unrecognizable when the period of oscillations becomes comparable to, or even smaller than, the spacing of discrete lines in the spectrum.

The bound–free portions of the spectra themselves immediately excluded the vibrational numbering in the  $c^3\Sigma^+$  state with  $v_0=12$  proposed by Katô *et al.*;<sup>7</sup> they already displayed too many peaks. A rough examination of the

TABLE I. The potential curve of the  $c^3\Sigma^+$  state in NaK obtained in the present work.

$R\text{ (nm)}$	$V\text{ (cm}^{-1}\text{)}$
0.33	17 729
0.34	17 289
0.35	16 959
0.36	16 689
0.37	16 470
0.38	16 293
0.39	16 153
0.40	16 045
0.41	15 965
0.42	15 910
0.43	15 875
0.44	15 859
0.445	15 857
0.45	15 858
0.46	15 872
0.47	15 906
0.48	15 959
0.49	16 020
0.50	16 090
0.51	16 166
0.52	16 248
0.53	16 335
0.54	16 424
0.55	16 514
0.56	16 604
0.57	16 694
0.58	16 781
0.59	16 866
0.60	16 947
0.61	17 024
0.62	17 097
0.63	17 165
0.64	17 230
0.65	17 291
0.66	17 351
0.67	17 408
0.68	17 459
0.69	17 509
0.70	17 556
0.71	17 601
0.72	17 644

bound–bound parts of the spectra led to the conclusion that in each case they contain three or four intensity maxima (see the insets in Figs. 2 and 3). This result supported our original vibrational assignment with  $v_0=16$  but it turned out to be misleading. In fact, in a simplistic picture, a spacing between the two adjacent maxima in the radial probability density, e.g., for  $v'=v_0+8$  in the  $c^3\Sigma^+$  state is around  $0.01\text{ nm}$ , whereas the distance between outer turning points of, for instance,  $v''=7$  and  $v''=8$  in the  $a^3\Sigma^+$  state is almost  $0.03\text{ nm}$ .<sup>12</sup> Therefore, it is obvious that the oscillations of the radial probability density for levels in the  $c^3\Sigma^+$  state cannot be reflected in a simple way on the intensity pattern of the discrete spectrum. To resolve this problem, we applied the method suggested by Tellinghuisen *et al.*,<sup>22</sup> which simplifies the treatment of the discrete region of the spectrum by artificially making it a part of the oscillatory continuum. For model calculations the  $a^3\Sigma^+$  state was treated as though it

TABLE II. Comparison of molecular constants for the  $c^3\Sigma^+$  state obtained by various authors. All quantities are in  $\text{cm}^{-1}$ , except  $R_e$  in nm. Note that  $T_e$  and  $D_e$  values are incongruous for some theoretical calculations, which results from deficiencies in the calculated positions of the atomic asymptote.

	$T_e$	$\omega_e$	$\omega_e x_e$	$D_e$	$R_e$
Experimental					
This work	$15\,857 \pm 15$	$63.17^a$	$0.1615^{a,b}$	$2461 \pm 15$	$0.445 \pm 0.001$
Ref. 3	15 719	75.5	0.56	2599	
Ref. 10	15 998.5	73.8	0.65	2319.3	0.410
Ref. 7	16 283.6	68.6	0.64	2034.2	0.426
Theoretical					
Ref. 27		63		2581	0.447
Ref. 28	16 675	122			0.449
Ref. 29	16 100	77		2097	0.434
Ref. 25	15 799	74.0	0.52	2645	0.424

<sup>a</sup>These constants represent positions of  $v'=20-40$ .

<sup>b</sup> $\omega_e y_e = -0.004\,18$ .

were completely repulsive, with  $V''(R) = V''(R_e)$  for  $R > R_e$  in place of the attractive branch. We found that the spectra of the  $c^3\Sigma^+ \rightarrow a^3\Sigma^+$  transition simulated using the “completely repulsive”  $a^3\Sigma^+$  state potential and those calculated with the “true”  $a^3\Sigma^+$  state potential are nearly identical in the range of the final state energies above the true dissociation limit (i.e., in the true bound-free part). Therefore, the number of intensity maxima contained in the true bound-bound part of the spectrum must be the same as observed in the corresponding part of the spectrum simulated with the completely repulsive  $a$  state potential, even if the positions of the latter are different. As shown in Figs. 2 and 3, the discrete parts of the spectrum contain, in fact, seven and nine maxima for excitation of  $v_0+5$  and  $v_0+13$  levels, respectively. As a result, to match the number of extrema in the vibrational wave function with the peaks in the observed spectra, the vibrational numbering in the  $c^3\Sigma^+$  state has to be changed by four quanta, giving  $v_0=20$ . This value matches also the number of maxima observed in all other spectra not shown here. The vibrational numbering inferred directly from the spectra is in agreement with the quantum mechanical calculations of eigenenergies for the constructed  $c^3\Sigma^+$  state potential. Table II compares the  $T_e$  and  $R_e$  of the  $c^3\Sigma^+$  state potential obtained in this work with the values proposed in previous experimental works and with the results of various theoretical approaches. The distinctive feature of the new potential is the larger value of the equilibrium distance  $R_e$  compared to values extrapolated from previous experimental observations as well as those resulting from the most recent calculations. This parameter turned out to be crucial to obtain the monotonic Mulliken difference potential for the  $c^3\Sigma^+ \rightarrow a^3\Sigma^+$  transition. We notice the large uncertainty,  $\pm 15\text{ cm}^{-1}$ , on the  $T_e$  value. It results partly from our limited spectral resolution,  $4\text{ cm}^{-1}$ , but is mainly due to the lack of precision inherent to the LeRoy’s inversion method.<sup>21</sup>

Fixing  $T_e = 15\,857\text{ cm}^{-1}$  and  $v_0=20$ , a fourth degree polynomial fitting of  $E_v$ , the energy of the vibrational levels for  $v'=20-40$ , obtained from our previous works,<sup>10,23</sup> allows us to deduce the vibrational spectroscopic constants  $\omega_e$ ,  $\omega_e x_e$ , and  $\omega_e y_e$  of the  $c^3\Sigma^+$  state (see Table II). For the

observed  $v$  levels, these constants locate the measured  $E_v$  within  $1\text{ cm}^{-1}$ . However, given the large uncertainty in  $T_e$ , the discrepancy can be several times larger for lower  $v$  levels. Likewise, fixing  $B_0=0.0588\text{ cm}^{-1}$ , deduced from  $R_e=0.445\text{ nm}$ , a third degree polynomial fitting of the measured  $B_v$  of  $v'=20-40$  levels,<sup>10,23</sup> gives  $\alpha=0.000\,30$  and  $\gamma=-7.4 \times 10^{-6}\text{ cm}^{-1}$ .

Having constructed the  $c^3\Sigma^+$  state potential curve we returned to the rigorous quantum mechanical simulations of the spectra. As expected, we obtained good overall agreement with the experimental observations, particularly in the positions of the intensity maxima and minima. The only noticeable difference was on the low frequency side of the spectra, where the first three peaks appeared a few tens of  $\text{cm}^{-1}$  too far apart in our simulations. As the transitions corresponding to these peaks are localized at small internuclear separations, slightly outside the range of validity of the  $a^3\Sigma^+$  state potential curve given by Masters *et al.*,<sup>14</sup> we attributed the observed discrepancy to the repulsive limb of the  $a^3\Sigma^+$  state potential being too steep. We were able to improve the agreement between the experimental and simulated spectra using the repulsive part of the  $a^3\Sigma^+$  state potential in the simple polynomial form

$$V(R) = 66\,154 - 371\,600R + 756\,650R^2 - 534\,200R^3 \quad (2)$$

( $V$  in  $\text{cm}^{-1}$ ,  $R$  in nm), valid for  $0.33\text{ nm} < R < 0.45\text{ nm}$ . This potential is virtually identical with that given by Masters *et al.*<sup>14</sup> except for the lowest  $R$  values,  $R < 0.35\text{ nm}$ . Figures 2 and 3 show the comparison of the experimental spectra with the simulations based on potentials presented earlier. It can be seen that the intensities of the simulated low frequency peaks are still too high. It must be remembered, however, that in all our calculations the  $c-a$  transition dipole moment  $\mu(R)$  has been assumed constant. Including the  $\mu(R)$  computed theoretically by Ratcliff *et al.*<sup>24</sup> made the comparison even worse; their transition dipole moment peaks at low  $R$  values, increasing the low frequency part of the spectrum. This result may suggest either a deficiency in the potential curves used, or in the theoretical  $\mu(R)$ . We

TABLE III. Observed vibrational variation of perturbation matrix elements (PME) compared to calculated overlap integrals (all sets of values normalized to 100 for  $v_{\Pi}=12 \sim v_{\Sigma}=v_0+15$ ,  $J=14$ ).

$v_{\Pi} \sim v_{\Sigma}$	$J$	PME observed		Overlap integrals, calculated	
		Ref. 5		Ref. 5	This work
$4 \sim v_0+5$	13	27		28	19
$6 \sim v_0+8$	33	38		42	28
$8 \sim v_0+10$	5	69		74	57
$8 \sim v_0+11$	46	46		51	38
$9 \sim v_0+12$	40	60		64	51
$10 \sim v_0+13$	33	76		78	66
$11 \sim v_0+14$	25	86		90	82
$12 \sim v_0+15$	14	100		100	100
		rms deviation		1.3	3.0
		absolute $ \langle v_{\Sigma}   v_{\Pi} \rangle $ for $12 \sim v_0+15$		0.062	0.0065

should note that the equilibrium distance of the  $c^3\Sigma^+$  state potential calculated by the same authors<sup>25</sup> is too small by 0.021 nm compared to the potential constructed in this work. A similar shift in the theoretical  $\mu(R)$  curve would improve the simulated spectra.

## DISCUSSION

It must be emphasized that the problem of vibrational numbering in the  $c^3\Sigma^+$  state of NaK has now been solved unambiguously, by the direct experimental observation. On the other hand, the  $c^3\Sigma^+$  state potential proposed in this paper is only sufficient to represent the gross structure of the bound-free  $c^3\Sigma^+ \rightarrow a^3\Sigma^+$  transition. It allows the energy eigenvalues to be predicted for given rovibrational levels with only limited accuracy and definitely cannot replace the need for high resolution experiments. Instead, it should be considered as a first approximation, a starting point for a more detailed study of the bottom of the  $c^3\Sigma^+$  state. For example, this could be done in a perturbation facilitated laser-induced fluorescence experiment,<sup>26</sup> where excitation of some high-lying molecular levels of NaK of a mixed singlet-triplet character could be followed by fluorescence to the  $c^3\Sigma^+$  state.

Having this in mind, we address the question of how our proposed  $c^3\Sigma^+$  state potential fits other experimental observations. In particular, the apparently wrong vibrational numbering in the  $c$  state (with  $v_0=16$ ) recommended before<sup>5</sup> was based on the study of the spin-orbit perturbation matrix element  $\xi$  between the  $c^3\Sigma^+$  and  $B^1\Pi$  states. It is known that  $\xi$  can be factored into an electronic part and a vibrational overlap integral  $\xi = \xi_{el} \langle v_{\Sigma} | v_{\Pi} \rangle$ , where  $|v_{\Sigma}\rangle$  and  $|v_{\Pi}\rangle$  are vibrational wave functions corresponding to the  $c^3\Sigma^+$  and  $B^1\Pi$  states. It was found that with the previous  $c$  state potential curve, the calculated overlap integrals correctly matched the observed variation of the perturbation matrix elements.<sup>5</sup> For the newly constructed  $c^3\Sigma^+$  state potential the agreement in relative values of overlap integrals is slightly worse but still acceptable (Table III). The problem lies in their absolute values which allow the electronic perturbation parameter  $\xi_{el}$  to be determined. The previous potential gives  $\xi_{el}=9 \text{ cm}^{-1}$ , the present one  $\xi_{el}=90 \text{ cm}^{-1}$ , to be compared with the estimate

based on the atomic spin-orbit parameter for  $K(4^2P)$ ,  $\xi_{el}=19 \text{ cm}^{-1}$ .<sup>10</sup> This shows once again the preliminary character of the  $c^3\Sigma^+$  state potential presented here. We believe that small changes of the  $c$  state equilibrium distance can considerably influence the overlap integrals discussed here, while leaving the  $c^3\Sigma^+ \rightarrow a^3\Sigma^+$  spectrum unchanged. However, as we cannot resolve this problem unambiguously, we shall not pursue it here.

## ACKNOWLEDGMENTS

We wish to thank Professor R. L. LeRoy and Professor W. C. Stwalley for making their computer programs BPOT and BOUND-FREE available for us.

- <sup>1</sup>J. Derouard and N. Sadeghi, Opt. Commun. **57**, 239 (1986).
- <sup>2</sup>R. F. Barrow, R. M. Clements, J. Derouard, N. Sadeghi, C. Effantin, J. d'Incan, and A. J. Ross, Can. J. Phys. **65**, 1154 (1987).
- <sup>3</sup>J. Derouard and N. Sadeghi, J. Chem. Phys. **88**, 2891 (1988).
- <sup>4</sup>J. Derouard, H. Debontride, T. D. Nguyen, and N. Sadeghi, J. Chem. Phys. **90**, 5936 (1989).
- <sup>5</sup>P. Kowalczyk, J. Derouard, and N. Sadeghi, J. Mol. Spectrosc. **151**, 303 (1992).
- <sup>6</sup>M. Baba, S. Tanaka, and H. Katô, J. Chem. Phys. **89**, 7049 (1988).
- <sup>7</sup>H. Katô, M. Sakano, N. Yoshie, M. Baba, and K. Ishikawa, J. Chem. Phys. **93**, 2228 (1990).
- <sup>8</sup>M. Baba, K. Nishizawa, N. Yoshie, K. Ishikawa, and H. Katô, J. Chem. Phys. **96**, 955 (1992).
- <sup>9</sup>P. Kowalczyk, B. Krüger, and F. Engelke, Chem. Phys. Lett. **147**, 301 (1988).
- <sup>10</sup>P. Kowalczyk, J. Chem. Phys. **91**, 2779 (1989).
- <sup>11</sup>K. Ishikawa, T. Kamauchi, M. Baba, and H. Katô, J. Chem. Phys. **96**, 6423 (1992).
- <sup>12</sup>A. J. Ross, C. Effantin, J. D'Incan, and R. F. Barrow, Mol. Phys. **56**, 903 (1985).
- <sup>13</sup>A. J. Ross and G. H. Jeung, Chem. Phys. Lett. **132**, 44 (1986).
- <sup>14</sup>M. Masters, J. Huennekens, W. T. Luh, Li Li, A. M. Lyyra, K. Sando, V. Zafropoulos, and W. C. Stwalley, J. Chem. Phys. **92**, 5801 (1990).
- <sup>15</sup>J. Cachena, C. Man, P. Cerez, A. Brillet, F. Stoeckel, A. Jourdan, and F. Hartmann, Rev. Phys. Appl. **14**, 685 (1979).
- <sup>16</sup>A. R. Striganov and N. S. Sventitskii, *Tables of Spectral Lines of Neutral and Ionized Atoms* (Plenum, New York, 1968).
- <sup>17</sup>J. W. Cooley, Math. Comput. **15**, 363 (1961).
- <sup>18</sup>P. S. Herman and K. M. Sando, J. Chem. Phys. **68**, 1153 (1978).
- <sup>19</sup>R. S. Mulliken, J. Chem. Phys. **55**, 309 (1971).
- <sup>20</sup>J. Tellinghuisen, Phys. Rev. Lett. **34**, 1137 (1975).

- <sup>21</sup>R. L. LeRoy, W. J. Keogh, and M. S. Child, *J. Chem. Phys.* **89**, 4564 (1988).
- <sup>22</sup>J. Tellinghuisen, A. Ragone, M. S. Kim, D. J. Auerbach, R. E. Smalley, L. Wharton, and D. H. Levy, *J. Chem. Phys.* **71**, 1283 (1979).
- <sup>23</sup>J. Derouard and N. Sadeghi (unpublished). For details see Ref. 3.
- <sup>24</sup>L. B. Ratcliff, D. D. Konowalow, and W. J. Stevens, *J. Mol. Spectrosc.* **110**, 242 (1985).
- <sup>25</sup>W. J. Stevens, D. D. Konowalow, and L. B. Ratcliff, *J. Chem. Phys.* **80**, 1215 (1984).
- <sup>26</sup>Li Li, S. F. Rice, and R. W. Field, *J. Chem. Phys.* **82**, 1178 (1985).
- <sup>27</sup>A. C. Roach, *J. Mol. Spectrosc.* **42**, 27 (1972).
- <sup>28</sup>R. Janoschek and H. U. Lee, *Chem. Phys. Lett.* **58**, 47 (1978).
- <sup>29</sup>G. H. Jeung, J. P. Daudey, and J. P. Malrieu, *Chem. Phys. Lett.* **94**, 300 (1983).